Thermodynamic-based model for the thermo-poro-elastoplastic behavior of saturated clay.

M.H. Sojoudi, Biao Li
Department of Building, Civil & Environmental Engineering, Concordia University, Montreal, Quebec, Canada

ABSTRACT
The thermo-poro-mechanical or thermo-hydro-mechanical (THM) coupling in clay related geomaterials is one of the most important issues in sustainable geotechnics. Clay soils have complex mineral composition and microstructure; thus, the study of thermo-poro-mechanical behavior is complicated. Previous studies shed little light on the difference between a thermal plastic strain and thermally induced dehydration behaviors. In this study, we propose a thermodynamic-based constitutive model for describing the thermo-poro-elastoplastic behavior of saturated clay. The proposed model considers the effect of temperature variation and mechanical loading on elastoplastic strains and dehydrations. The thermo-mechanical behavior is captured by using the thermodynamics laws and subloading surface plasticity. The hardening rule is established by using laws of physical conservation, energy dissipation and plastic flow. Dehydration behavior is considered using the laws of thermodynamics for chemical processes. A comparison between model predictions and experimental data for some clay soils with different geological origins is presented and a reasonable result is achieved.

RÉSUMÉ
Le couplage thermo-poro-mécanique ou thermo-hydro-mécanique (THM) dans les géomatériaux liés à l'argile est l'un des enjeux les plus importants de la géotechnique durable. Les sols argileux ont une composition minérale et une microstructure complexes; ainsi, l'étude de la thermo-poro-mécanique est compliquée. Des études antérieures ont peu éclairé la différence entre la déformation plastique thermique et les comportements de déshydratation induite thermiquement. Dans cette étude, nous proposons un modèle constitutif thermodynamique pour décrire le comportement thermo-poro-élastoplastique de l'argile saturée. Le modèle proposé tient compte de l'effet de la variation de température, de la charge mécanique et du taux de charge sur les déformations élastoplastiques et les déshydrations. Le comportement thermo-mécanique est capturé en utilisant les lois de la thermodynamique et la sous-charge de la plasticité de la surface. La règle de durcissement est établie en utilisant des lois de conservation physique, de dissipation d'énergie et d'écoulement plastique. Le comportement de déshydratation est considéré en utilisant les lois de la thermodynamique pour les processus chimiques. Une comparaison entre les prédictions du modèle et les données expérimentales pour certains sols argileux de différentes origines géologiques est présentée et un résultat raisonnable est obtenu.

1 INTRODUCTION

Over the past decades, many experimental tests and studies showed that the variation of the temperature has a significant effect on the mechanical behavior of hydrated clay (Laloui and Cekerevac, 2008; Monfared et al., 2012). Change of temperature has a couple of effects on the mechanical and hydraulic behavior of clayey materials which this behavior is known as one of the major issues in geotechnical engineering. There are many executions related to the thermo-elastic-viscoplastic behavior of hydrated clay which has adverse effects on the stability of clayey materials, for instance, the increasing of the temperature induced by the deep disposal of nuclear waste (Laloui and Modaressi, 2002; Monfared et al. 2012) and energy pile foundations (You et al., 2014; Akrouch et al. 2014).

Previous experimental results show that the thermo-mechanical behavior of clay soil is a function of the OCR (over-consolidation ratio). When a clay soil is heated, all of its particles dilates. However, an increase of temperature decreases the strength of adsorbed layers which leads to a decrease of the distance between clay particles. According to Mitchell (1976), under the normally consolidated condition, this behavior changes the

equilibrium between the Van der Waals attractive forces and the electrostatic repulsive forces, which causes grain rearrangement and shrinkage. On the other hand, when a high OCR clay soil is heated, it mainly fabricates reversible thermal expansion. According to studies by Cekerevac and Laloui (2004) and Laloui and François (2009), the inclination of the soil towards dilation and contraction and intensity of the reversible/irreversible parts of the deformation under cycle of heating and cooling relates upon clayey materials types, OCR and plasticity.

In addition to what was mentioned above, the exact thermo-poro-mechanical behavior of clayey materials is still under debate and a comprehensive conclusion has not been reached yet. On one hand, many experimental and numerical works showed that the increase of temperature would decrease the clayey material's strength, and, in some cases, thermal failure had been reported (Monfared et al. 2012; Hueckel et al. 2009). On the other hand, works done by (Zhang et al.2012; Laloui and Cekerevac 2008; Kuntiwattanakul et al.1995) showed that the increase of temperature will increase the shear strength of clay materials.

To simulate these behaviors of soil, plasticity-based models were increasingly proposed by researchers to characterize the thermo-plastic behavior. The plasticity-based models consider the effect of temperature on the yield surface, plastic potential, hardening-softening parameters and flow rule (Gao et al. 2009; Okada 2005; Hueckel et al. 2009; Xiao 2014; Ghasemzadeh et al. 2017). Masín and Khalili (2012) proposed a model coupled the thermal behavior of soils with elastoplastic constitutive models. Laloui and Cekerevac (2008) developed a multi-yield surface model based on Cam-Clay plasticity for considering the effects of cyclic shear loading. Zhang et al. (2012) and Xiong et al. (2017), based on the assumption that the geomaterials are a continuous media, proposed the concept of "temperature-deduced equivalent stress" into their thermo-mechanical model for considering the effect of temperature on the evolution of the yield surface. However, those above-mentioned models cannot comprehensively predict the thermal contraction behavior due to clay dehydration. This phenomenon is caused by breakdown of bounding water when soils are heated (Monfared et al. 2012). In addition, since the temperature of soils changes periodically and increasing the cycle of heating-cooling will increase the accumulation of the shear stress reduction and irreversible deformation of soils (Bai et al., 2014), the proposed models should have the ability to simulate the soil behavior under heating and cooling cycles. As mentioned above, simulating the soil's behavior under cycles of wetting-drying, heating-cooling and loading-unloading are very complex. Thus, presenting a comprehensive model to consider this complex coupled behavior under cyclic loading base on the classical plasticity theory is very challenging.

In this research a comprehensive, thermo-poro-elastoplastic constitutive model based on thermodynamics theory and unconventional plasticity for a range of saturated clays is presented. The model is capable of considering the influence of the temperature variation on the mechanical behavior and dehydration processes.

2 THERMO-PORO-MECHANICAL FRAMEWORK

The selection of appropriate stress and strain variables is an essential step for developing the constitutive thermo-mechanical model for geomaterials. As was demonstrated by Voyiadjis and Abu Al-Rub (2003), Helmholtz free energy Ψ can be given as a function of the elastic strain ε_{ij}^{e} ,temperature *T* and volumetric *plastic* strain *P*. In addition, in this study we considerd apparent density of bounding water ρ^{b} as a function of Helmholtz free energy Ψ as well.

$$\Psi = \Psi(\varepsilon_{ij}^{e}, T, P, \rho^{b}) \quad [1]$$

According to the fundamentals of thermodynamics and plasticity the Clausius-Duhem inequality and total strain equation can be write as below,

$$\sigma_{ij}\dot{\varepsilon}_{ij} - \rho(\dot{\Psi} + S\dot{T}) - q_i \frac{T_i}{T} \geq 0 \quad [2]$$

$$\dot{\boldsymbol{\varepsilon}}_{ij} = \dot{\boldsymbol{\varepsilon}}_{ij}^{e} + \dot{\boldsymbol{\varepsilon}}_{ij}^{p} \quad [3]$$

By taking the time derivation of Helmholtz free energy (Equation 1) in respect to its state variables, Equation 4 implies as ,

$$\dot{\Psi} = \frac{\partial \Psi}{\partial \varepsilon_{ij}^{e}} \dot{\varepsilon}_{ij}^{e} + \frac{\partial \Psi}{\partial T}\dot{T} + \frac{\partial \Psi}{\partial P}\dot{P} + \frac{\partial \Psi}{\partial \rho^{b}}\dot{\rho}^{b} \quad [4]$$

where by substituting Equation 4 into Equation 2 and making use of Equation 3 the following thermodynamic inequality is postulated.

$$(\sigma_{ij} - \rho\frac{\partial \Psi}{\partial \varepsilon_{ij}^{e}})\dot{\varepsilon}_{ij}^{e} + \sigma_{ij}\dot{\varepsilon}_{ij}^{p} - \rho(\frac{\partial \Psi}{\partial T} + S)\dot{T} - \rho\frac{\partial \Psi}{\partial P}\dot{P} - q_i\frac{T_i}{T} - \rho\frac{\partial \Psi}{\partial \rho^{b}}\dot{\rho}^{b} \geq 0 \quad [5]$$

By using the equation 5 and base on the fact that Clausius-Duhem inequality is valid for all loading histories, thermodynamics conjugate forces and state laws can be described as below,

$$\sigma_{ij} = \rho\frac{\partial \Psi}{\partial \varepsilon_{ij}^{e}}; S = -\frac{\partial \Psi}{\partial T}; H = \rho\frac{\partial \Psi}{\partial P}; L = \rho\frac{\partial \Psi}{\partial \rho^{b}} \quad [6]$$

where *S* is the soil entropy, *H* is the conjugate force of volumetric strain and *L* is the conjugate force of the apparent density of bounding water.

2.1 Specific free energy function.

According to Equation 1, In this study, it is assumed that the Helmholtz free energy can be written as a consist of thermo-elastic Ψ^{te},thermo-plastic Ψ^{tp} and dehydration Ψ^{Deh} components.

$$\Psi = \Psi^{te}(\varepsilon_{ij}^{e}, T) + \Psi^{tp}(P, T) + \Psi^{Deh}(\rho^{b}, T) \quad [7]$$

Based on Voyiadjis and Abu Al-Rub (2003), Darabi.et al. (2012), Zhang (2017) and the definition of Helmholtz free energy, the thermo-elastic, thermo-plastic and dehydration parts of total Helmholtz free energy are defined as:

$$\rho\Psi^{te}(\varepsilon_{ij}^{e}, T) = (\varepsilon_{ij} - \varepsilon_{ij}^{p}) E_{ijkl} v^{e}(T) (\varepsilon_{kl} - \varepsilon_{kl}^{p}) \quad [8]$$

$$\rho\Psi^{tp}(P, T) = (H_0(\rho - \gamma)\exp(\frac{p}{\rho - \gamma})) v^{P}(T) \quad [9]$$

$$\rho\Psi^{Deh}(\rho^{b}, T) = e_b - TS^{b} \quad [10]$$

ε_{ij}^{e} is elastic strain,H_0 is the initial value of H, e_b and S^b are the internal energy and the specific entropy of bound water, respectively.

$v^{e}(T), v^{p}(T)$ are the Arrhenius- type temperature term for coupling temperature to the elastic and plastic parts of Helmholtz free energy respectively. According to Darabi et al. (2012) it can be written as,

$$v^{e}(T) = v^{p}(T) = \exp[-\delta(1 - \frac{T}{T_0})] \quad [11]$$

In order to describe the plastic behavior, one needs to define first the plastic dissipation energy (Simo JC. 1998).

,

$$\Pi = \sigma_{ij}\dot{\varepsilon}_{ij}^{p} - H\dot{P} \geq 0 \quad [12]$$

By defining the Lagrange plastic multiplier $\dot{\lambda}$ and the normal yield surface function *f*, the objective function is given as:

$$\Omega = \Pi - \dot{\lambda} f \quad [13]$$

In order to obtain the inelastic dissipation function over all the possible states, the objective function should be maximized, where,

$$\frac{\partial\Omega}{\partial\sigma_{ij}} = 0, \quad \frac{\partial\Omega}{\partial H} = 0 \quad [14]$$

And, therefore,

$$\varepsilon_{ij}^{P} = \dot{\lambda}\frac{\partial f}{\partial\sigma_{ij}}, \dot{p} = -\dot{\lambda}\frac{\partial f}{\partial H} \quad [15]$$

3 ELASTOPLASTIC CALCULATIONS

By considering the Equation 7 and based on the work done by Li and Wong (2017) in this study it is assumed that the strain increment ($d\boldsymbol{\varepsilon}$) is additively decomposed into thermo-elastic, thermo-plastic and dehydration parts.

$$d\boldsymbol{\varepsilon} = d\boldsymbol{\varepsilon}^{te} + d\boldsymbol{\varepsilon}^{tp} + d\boldsymbol{\varepsilon}^{deh} \quad [16]$$

Where according to Equations 5, 6 and 16 total rate of energy dissipation can be decomposed into thermo-elastic $(\sigma_{ij} - \rho\frac{\partial\Psi^{te}}{\partial\varepsilon_{ij}^{e}})d\boldsymbol{\varepsilon}_{ij}^{te}$,thermo-plastic $\sigma_{ij}d\boldsymbol{\varepsilon}_{ij}^{tp} - \rho\frac{\partial\Psi^{tp}}{\partial P}\dot{p}$ and dehydration $\rho\frac{\partial\Psi^{deh}}{\partial\rho^{b}}d\boldsymbol{\varepsilon}_{ij}^{deh}$ components.

3.1 Thermo-elastic strain.

Thermo elastic behavior can be obtain from Equations 6 and 8 as below,

$$\sigma_{ij} = E_{ijkl}(\varepsilon_{kl} - \varepsilon_{kl}^{p}) v^{e(T)} \quad [17]$$

where E_{ijkl} is fourth-order stiffness tensor.

3.2 Thermo-plastic strain.

In this model the plastic deformation is calculated within the subloading surface elastoplasticity framework (Hashiguchi et al. 2002). In this framework, the constitutive equations are derived based on introduction of LC (Loading Collapse) normal yield surface and subloading surface. The LC normal yield surface is the renamed form of the conventional LC yield curve, while its interior is not regarded as a purely elastic domain. The subloading surface is introduced as a surface which always passes through the current stress point, while keeping a similar shape to the LC normal yield surface with respect to the origin of the stress space:

$$f(\boldsymbol{\sigma}) = RH(P) \quad [18]$$

where R is the similarity ratio of the subloading surface to the LC normal yield surface. This ratio is called the normal yield ratio. Differentiating Equation 18 results in:

$$\left(\frac{\partial f(\boldsymbol{\sigma})}{\partial\boldsymbol{\sigma}}\right)^{T} d\boldsymbol{\sigma} = HdR + RH'\dot{P} \quad [19]$$

The evolution of the normal yield ratio could be described as (Hashiguchi et al. 2002):

$$dR = U\left\|d\varepsilon^{p}\right\| \text{ for } d\varepsilon^{p} \neq 0 \quad [20]$$

where *U* is monotonically decreasing function of *R* that should satisfy the following conditions:

$$\begin{aligned} &U = +\infty \text{ for } R = 0 \\ &U = 0 \quad \text{for } R = 1 \\ &U < 0 \quad \text{for } R > 1 \end{aligned} \quad [21]$$

These conditions are required to guarantee that the subloading surface approaches the normal yield surface during a loading process. The equation satisfying

conditions (Equation 21) is described by Hashigushi et al. (2002):

$$U = -u \ln R \quad [22]$$

where *u* is a material parameter.
Moreover, according to Equations 6 and 9,

$$H(p) = \rho \frac{\partial \Psi^p}{\partial p} = (H_0 \exp(\frac{p}{\rho - \gamma}))v^p(T) \quad [23]$$

$$H' = \frac{H}{\rho - \gamma} \quad [24]$$

Substituting Equations 20 and 24 into Equation 19, one obtains:

$$\left(\frac{\partial f(\boldsymbol{\sigma})}{\partial \boldsymbol{\sigma}}\right)^T d\boldsymbol{\sigma} = U \left\| d\boldsymbol{\varepsilon}^p \right\| H + RH'\dot{P} \quad [25]$$

According to Equation 15 and assuming the associated flow rule:

$$d\boldsymbol{\varepsilon}^p = \dot{\lambda}\overline{\mathbf{N}} \quad [26]$$

Where $\dot{\lambda}$ is the positive proportionality factor, and the vector $\overline{N}$ is the unit normal vector of the subloading surface at the current stress point:

$$\overline{\mathbf{N}} = \frac{\partial f(\boldsymbol{\sigma})}{\partial \boldsymbol{\sigma}} \Big/ \left\| \frac{\partial f(\boldsymbol{\sigma})}{\partial \boldsymbol{\sigma}} \right\| \quad [27]$$

Substitution of Equation 26 into Equation 25 leads to:

$$\dot{\lambda} = \frac{\overline{\mathbf{N}}^T d\boldsymbol{\sigma}}{M^P} \quad [28]$$

Where

$$M^P = (\frac{U}{R} + \frac{H'}{H}\overline{h}) \quad [29]$$

$$\overline{h} = \frac{\dot{p}}{\dot{\lambda}} \quad [30]$$

Based on the loading criterion proposed by Hashiguchi et al. (2002), the loading criterion in the proposed model is given by:

$$\begin{aligned} tr(\overline{N}Ed\varepsilon) > 0 &\rightarrow d\boldsymbol{\varepsilon}^p \neq 0 \\ tr(\overline{N}Ed\varepsilon) \leq 0 &\rightarrow d\boldsymbol{\varepsilon}^p = 0 \end{aligned} \quad [31]$$

3.3 Dehydration strain.

Base on the definition of the apparent density of bounding water it can be written as,

$$\rho^b = \rho_b \phi_b, \quad \phi_b = \frac{v_b}{v} \quad [32]$$

Where ρ_b, ϕ_b, v_b and v are the corresponding intrinsic densities of bounding water, volume fraction of bounding water, volume of bounding water and total volume of soil respectively. By differentiating Equation 32, the increment of apparent density of bounding water can be given as:

$$d\rho^b = \rho_b (\frac{dv_b}{v} + \phi_b d\varepsilon_v) \quad [33]$$

According to the definition of dehydration strain by Li and Wong (2017), Equation 33 can be written as,

$$d\rho^b = \rho_b d\varepsilon^{Deh} + \rho_b \phi_b d\varepsilon_v \quad [34]$$

Based on the works done by Li and Wong (2017), and Zhang (2017),it's assumed that the increment of apparent density of bounding water has a linear relation with its conjugate force.

$$d\rho^b = \rho \alpha_{bf} \frac{\partial \Psi_b}{\partial \rho^b} \quad [35]$$

Where ρ and α_{bf} are the total density of the soil and mass of free water converted from per unit mass of bound water per unit rise in temperature respectively.

By substituting Equation 34 into Equation 35, dehydration strain increment can be written as,

$$d\varepsilon^{Deh} = \frac{\rho}{\rho_b} \alpha_{bf} \frac{\partial \Psi_b}{\partial \rho^b} - \phi_b d\varepsilon_v \quad [36]$$

According to Equation 11 and Zhang (2017), the internal dehydration energy can be written as,

$$e_b = T\upsilon_b + \vartheta_b \quad [37]$$

$$\upsilon_b = \frac{S^b}{\rho^b} \quad [38]$$

$$\vartheta_b = (1 - \frac{K_m}{K_s\phi_s + K_b\phi_b}) \frac{\sigma_u \phi_s}{\rho^b} + \rho^b \frac{\partial(\omega_e^b / \rho^b)}{\partial \rho^b} \quad [39]$$

Where K_m is the bulk modulus of soil skeleton; K_s and K_b are the intrinsic bulk moduli of soil particles and bound water, respectively. σ_u is the pore water pressure.

ω_e^b is defined as,

$$\omega_e^b = f_b(\rho^b)[E_v^{e\beta+2} + \xi(E_v^e + c)^\beta \varepsilon_s^{e2}] \quad [40]$$

1 Materials parameters involved in the model.

References	Description	υ	m	ρ	γ	u	σ' (MPa)	$\alpha_{bf}(^{\circ}c^{-1})$	$\beta_T(^{\circ}c^{-1})$	B_b	K_b	ξ
Li and Wong (2017)	Natural soft Mudrock	0.3	1.2	0.045	0.002	35	2.8	0.03	-2e-5	0.001	0.3	0.46
Del Olemo (1996)	Boom clay	0.1	1.8	0.2	0.001	10	1-6	0.02	-2e-5	0.001	0.3	0.7
Abuel-Naga (2005)	Bangkok clay	0.37	0.8	0.17	0.009	30	0.3	0.02	-2e-5	0.0001	0.1	0.3

Where

$$f_b(\rho^b) = B_b(\rho^b)^{k_b} \quad [41]$$

$$E_v^e = \varepsilon_v^e + \beta_T \Delta T;\ \varepsilon_s^e = \sqrt{e_{ij}^e e_{ij}^e},\ e_{ij}^e = \varepsilon_{ij}^e - \frac{\varepsilon_v^e}{3}\delta_{ij} \quad [42]$$

β is a power exponent that is taken as 1 in this study and β_T is the elastic thermal expansion coefficient of soil skeleton. ξ is a material constant; B_b and K_b are parameters accounting for the effect of bound water on the soil modulus. According to the Equations 10 and 37, the derivation of Helmholtz free energy over derivation of bonding water density can be postulated as,

$$\frac{\partial \Psi_b}{\partial \rho^b} = \frac{-T\upsilon_b}{\rho_b} + B_b(k^b - 1)^2(\rho^b)^{(k^b-2)}[E_v^{e\beta+2} + \xi(E_v^e + c)^\beta \varepsilon_s^{e2}] \quad [43]$$

Equation 43 shows the effect of temperature variation and mechanical loading on the change of dehydration strain.

4 COMPARISON WITH EXPERIMENTS

The ability of the proposed model in describing the thermo-poro-mechanical behavior of Natural soft Mudrock, Boom Clay and Bangkok Clay under the drain stress path condition are presented herein.

4.1 Determination of material parameters

In the proposed model, six stress-strain parameters (υ, m, H_0, ρ, γ, u) and five thermo-dehydration parameters (α_{bf}, β_T, B_b, K_b, ξ) are required to describe the thermo-poro-mechanical behavior of a clay soil. A common drained shear stress test at the saturated state of the soil can be used for determining the Poisson's ratio (υ) and the slope of the critical state line (m). The parameters H_0, ρ, γ which respectively indicate the pre-consolidation pressure, the slope of the normal consolidation line in $\ln v - \ln p$ plane and the slopes of swelling lines in $\ln v - \ln p$ plane. The parameter *u* does not have a clear physical meaning and mathematically stands to adjust the curvature of the stress–strain diagram. This parameter can be found by a trial-and-error procedure to fit the curvature of the soil behavior in its transitional state in stress- strain space. The value of α_{bf} and β_T can be found by using thermal consolidation test. The parameter B_b can be determined by performing isotropic compression test and the value of K_b and ξ can be found by using critical state data of soil.

4.2 Natural soft Mudrock and Boom Clay

Li and Wong (2017) and Del Olemo et al. (1996) reported the results of some drained triaxial tests on samples of Natural soft mudrock and Boom clay, respectively. The natural soft mudrock contains the mixture of illite-smectite for clay part and with the composition of quartz and a small amount of heavy mineral for the non-clay part. The Boom clay has a plasticity index of about 50%, a natural porosity around 40%, and a water content varying between 24% and 30%. The material parameters that were used to predict these soil behaviors are listed in table 1. Figure 1 and Figure 2 show the comparison of measured results and model predictions of Natural soft mudrock and Boom clay under temperature variation, respectively.

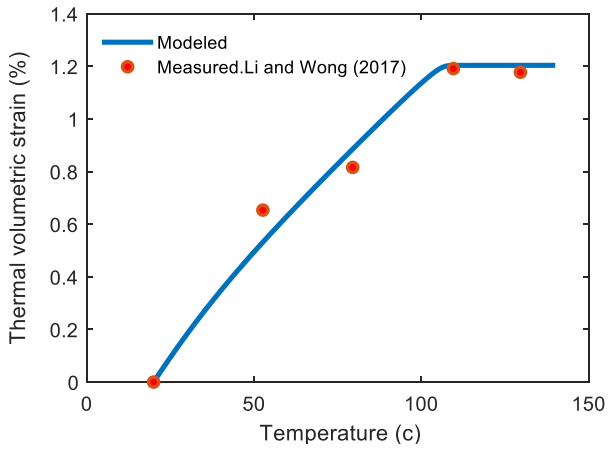

Figure 1. Comparison of model results and test data for thermal volumetric behavior of Natural soft Mudrock.

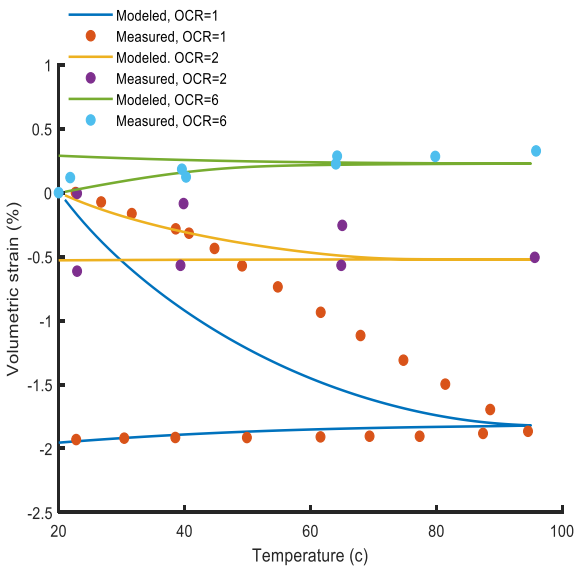

Figure 2. Comparison of model results and test data (Del Olemo et al. 1996) for thermal volumetric behavior of Boom Clay.

4.3 Bangkok Clay

Bangkok Clay is another soil which is used to validate the proposed model. Abuel-Naga (2005) conducted a series of drained triaxial loading tests on this soil. Figure 3 to Figure 8 shows the test results and model predictions for a drained triaxial test under a confining pressure of 300 kPa at 25°c, 70°c and 90 °c.The material parameters that were used to predict the soil behavior are listed in table 1.

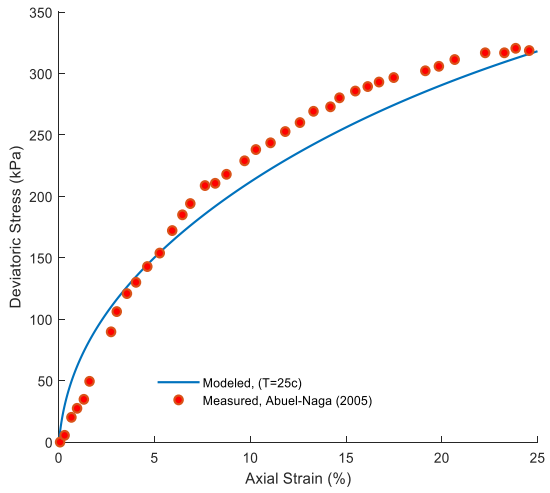

Figure 3. Comparison of model results and test data for drained triaxial compression test on NC Bangkok Clay ($P_0' = 300\ kPa$,Temperature = 25℃).

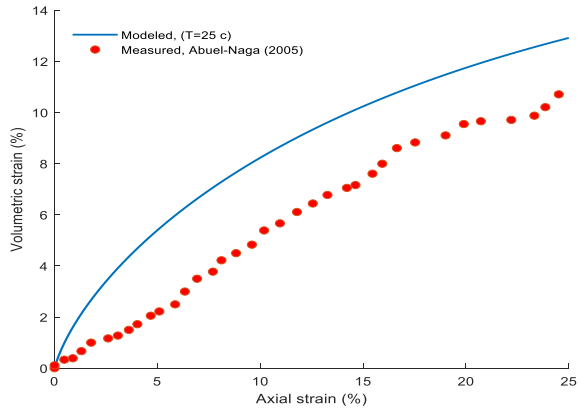

Figure 4. Comparison of model results and test data for drained triaxial compression test on NC Bangkok Clay ($P_0' = 300\ kPa$,Temperature = 25℃).

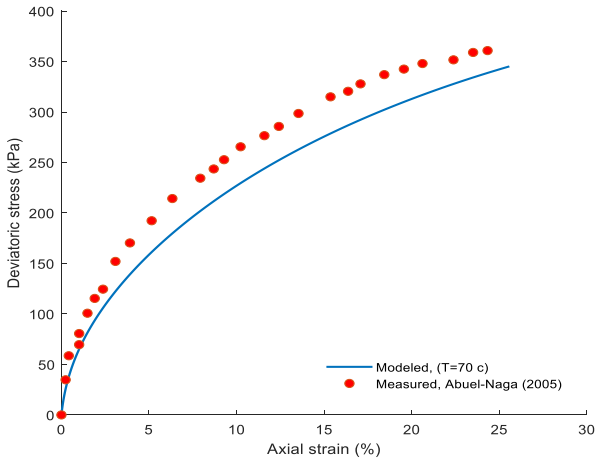

Figure 5. Comparison of model results and test data for drained triaxial compression test on NC Bangkok Clay ($P_0' = 300\ kPa$,Temperature = 70℃).

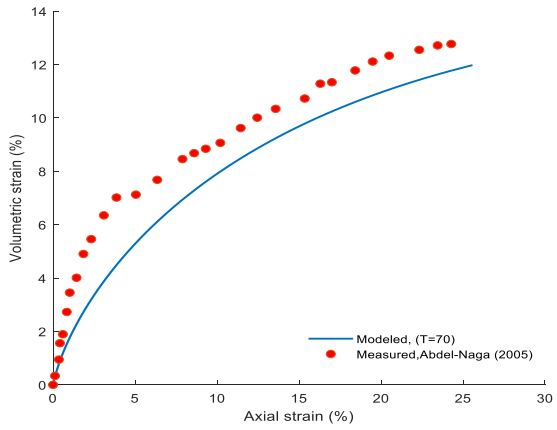

Figure 6. Comparison of model results and test data for drained triaxial compression test on NC Bangkok Clay ($P_0' = 300\ kPa$,Temperature = 70℃).

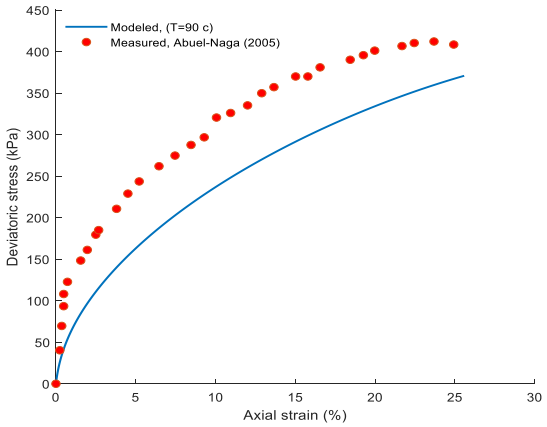

Figure 7. Comparison of model results and test data for drained triaxial compression test on NC Bangkok Clay ($P_0' = 300\ kPa$,Temperature = 90℃).

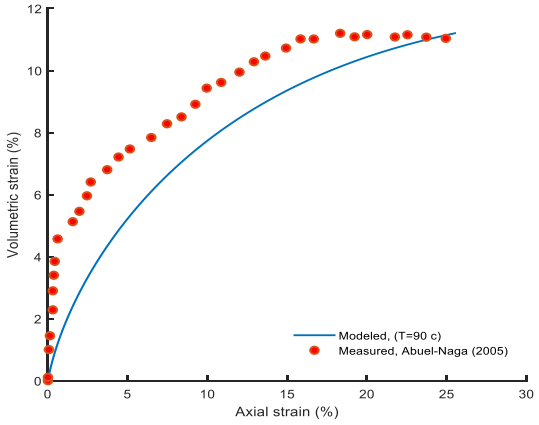

Figure 8. Comparison of model results and test data for drained triaxial compression test on NC Bangkok Clay. ($P_0' = 300\ kPa$,Temperature = 90℃)

5 CONCLUSIONS

In this paper, a thermo-poro-elastoplastic constitutive model based on the thermodynamics laws is presented to describe the coupled thermo-poro-mechanical behavior of saturated clay soils.

In the proposed model, subloading surface plasticity and thermodynamics laws are employed to describe the nonlinear thermomechanical and dehydration behavior of clayey materials. Since the selected mechanical framework considers the elastic-plastic domain inside of the yield surface, the proposed model describes the smooth elastic-plastic transition.

The dehydration induced strain behavior was treated separated and was characterized using Helmholtz free energy and energy dissipation functions.

Smooth and realistic predictions are two essential requirements for numerical modeling of coupled hydro-thermomechanical problems. It is applied to predict the thermo-poro-mechanical behavior of a natural soft mudrock, Boom Clay, and Bangkok Clay and thus, the capability of the model was verified.

6 REFRENCES

Abuel-Naga, H.M., 2006. Thermo-mechanical behavior of soft Bangkok clay: experimental results and constitutive modeling. D. Eng. Dissertation.

Akrouch, G.A., Sánchez, M. and Briaud, J.L., 2014. Thermo-mechanical behavior of energy piles in high plasticity clays. Acta Geotechnica, 9(3), pp.399-412.

Al-Rub, R.K.A. and Kim, S.M., 2009. Predicting mesh-independent ballistic limits for heterogeneous targets by a nonlocal damage computational framework. Composites Part B: Engineering, 40(6), pp.495-510.

Bai, B., Guo, L. and Han, S., 2014. Pore pressure and consolidation of saturated silty clay induced by progressively heating/cooling. Mechanics of Materials, 75, pp.84-94.

Cekerevac, C. and Laloui, L., 2004. Experimental study of thermal effects on the mechanical behaviour of a clay. International journal for numerical and analytical methods in geomechanics, 28(3), pp.209-228.

Čekerevac, C., 2003. Thermal effects on the mechanical behaviour of saturated clays: an experimental and constitutive study (Doctoral dissertation, Verlag nicht ermittelbar).

Darabi, M.K., Al-Rub, R.K.A., Masad, E.A. and Little, D.N., 2012. Thermodynamic-based model for coupling temperature-dependent viscoelastic, viscoplastic, and viscodamage constitutive behavior of asphalt mixtures. International Journal for Numerical and Analytical Methods in Geomechanics, 36(7), pp.817-854.

Del Olmo, C., Fioravante, V., Gera, F., Hueckel, T., Mayor, J.C. and Pellegrini, R., 1996. Thermomechanical properties of deep argillaceous formations. Engineering Geology, 41(1-4), pp.87-102.

Drucker, D.C. and Prager, W., 1952. Soil mechanics and plastic analysis or limit design. Quarterly of applied mathematics, 10(2), pp.157-165.

Gao, X., Zhang, T., Hayden, M. and Roe, C., 2009. Effects of the stress state on plasticity and ductile failure of an aluminum 5083 alloy. International Journal of Plasticity, 25(12), pp.2366-2382.

Ghasemzadeh, H., Sojoudi, M.H., Amiri, S.G. and Karami, M.H., 2017. Elastoplastic model for hydro-mechanical behavior of unsaturated soils. Soils and Foundations, 57(3), pp.371-383.

Hashiguchi, K., Saitoh, K., Okayasu, T. and Tsutsumi, S., 2002. Evaluation of typical conventional and unconventional plasticity models for prediction of softening behaviour of soils. Geotechnique, 52(8), pp.561-578.

Helwany, S., 2007. Applied soil mechanics with ABAQUS applications. John Wiley & Sons.

Houlsby, G.T. and Puzrin, A.M., 2000. A thermomechanical framework for constitutive models for rate-independent dissipative materials. International journal of Plasticity, 16(9), pp.1017-1047.

Hu, R., Chen, Y.F., Liu, H.H. and Zhou, C.B., 2015. A coupled stress–strain and hydraulic hysteresis model for unsaturated soils: thermodynamic analysis and model evaluation. Computers and Geotechnics, 63, pp.159-170.

Hueckel, T., François, B. and Laloui, L., 2009. Explaining thermal failure in saturated clays. Géotechnique, 59(3), pp.197-212.

Kuntiwattanakul, P., Towhata, I., Ohishi, K. and Seko, I., 1995. Temperature effects on undrained shear characteristics of clay. Soils and Foundations, 35(1), pp.147-162.

Laloui, L. and Cekerevac, C., 2008. Numerical simulation of the non-isothermal mechanical behaviour of soils. Computers and Geotechnics, 35(5), pp.729-745.

Laloui, L. and Modaressi, H., 2002. Modelling of the thermo-hydro-plastic behaviour of clays. Hydromechanical and Thermohydromechanical Behaviour of Deep Argillaceous Rock. Sous la direction de Hoteit, Su, Tijani et Shao, pp.161-170.

Laloui, L. and François, B., 2009. ACMEG-T: soil thermoplasticity model. Journal of engineering mechanics, 135(9), pp.932-944.

Laloui, L., 2001. Thermo-mechanical behaviour of soils. Revue française de génie civil, 5(6), pp.809-843.

Laloui, L., Leroueil, S. and Chalindar, S., 2008. Modelling the combined effect of strain rate and temperature on one-dimensional compression of soils. Canadian Geotechnical Journal, 45(12), pp.1765-1777.

Lebon, G., Jou, D. and Casas-Vázquez, J., 2008. Understanding non-equilibrium thermodynamics (Vol. 295). Berlin: Springer.

Li, B. and Wong, R.C., 2017. A mechanistic model for anisotropic thermal strain behavior of soft mudrocks. Engineering Geology, 228, pp.146-157.

Mašín, D. and Khalili, N., 2012. A thermo-mechanical model for variably saturated soils based on hypoplasticity. International journal for numerical and analytical methods in geomechanics, 36(12), pp.1461-1485.

Mitchell, J.K., 1993, Fundamentals of Soil Behavior, John Wiley and Sons, Inc., New York.

Monfared, M., Sulem, J., Delage, P. and Mohajerani, M., 2012. On the THM behaviour of a sheared Boom clay sample: Application to the behaviour and sealing properties of the EDZ. Engineering Geology, 124, pp.47-58.

Okada, T., 2005. Mechanical properties of sedimentary soft rock at high temperatures. part 1. Evaluation of temperature dependency based on triaxial compression test. Denryoku Chuo Kenkyusho Hokoku, pp.1-4.

Qiao, Y. and Ding, W., 2017. ACMEG-TVP: A thermoviscoplastic constitutive model for geomaterials. Computers and Geotechnics, 81, pp.98-111.

Simo, J.C., 1998. Numerical analysis and simulation of plasticity. Handbook of numerical analysis, 6, pp.183-499.

Voyiadjis, G.Z., Al-Rub, R.K.A. and Palazotto, A.N., 2004. Thermodynamic framework for coupling of non-local viscoplasticity and non-local anisotropic viscodamage for dynamic localization problems using gradient theory. International Journal of Plasticity, 20(6), pp.981-1038.

Voyiadjis, G.Z. and Al-Rub, R.K.A., 2003. Thermodynamic based model for the evolution equation of the backstress in cyclic plasticity. International Journal of Plasticity, 19(12), pp.2121-2147.

Xiao, H., 2014. Thermo-coupled elastoplasticity models with asymptotic loss of the material strength. International Journal of Plasticity, 63, pp.211-228.

Xiong, Y.L., Ye, G.L., Zhu, H.H., Zhang, S. and Zhang, F., 2017. A unified thermo-elasto-viscoplastic model for soft rock. International Journal of Rock Mechanics and Mining Sciences, 93, pp.1-12.

You, S., Cheng, X., Guo, H. and Yao, Z., 2014. In-situ experimental study of heat exchange capacity of CFG pile geothermal exchangers. Energy and Buildings, 79, pp.23-31.

Zhang, S., Leng, W., Zhang, F. and Xiong, Y., 2012. A simple thermo-elastoplastic model for geomaterials. International Journal of Plasticity, 34, pp.93-113.

Zhang, Z., 2017. A thermodynamics-based theory for thethermo-poro-mechanical modeling of saturated clay. International Journal of Plasticity, 92, pp.164-185.